SPANDIDOS
PUBLICATIONS

Ciprofloxacin promotes polarization of CD86⁺CD206⁻ macrophages to suppress liver cancer

MENGTIAN FAN[1*], SICHENG CHEN[2*], YAGUANG WENG[1], XIAN LI[3],
YINGJIU JIANG[2], XIAOWEN WANG[2], MENGJUN BIE[2], LIQIN AN[1], MENGHAO ZHANG[1],
BIN CHEN[1], GAIGAI HUANG[1], JINGHONG WU[1], MENGYING ZHU[1] and QIONG SHI[1]

[1]Ministry of Education Key Laboratory of Diagnostic Medicine, School of Laboratory Medicine;
Departments of [2]Cardiothoracic Surgery and [3]Pathology, The First Affiliated Hospital,
Chongqing Medical University, Chongqing 400016, P.R. China

Abstract. Gut microbiota can promote tumor development by producing toxic metabolites and inhibiting the function of immune cells. Previous studies have demonstrated that gut microbiota can reach the liver through the circulation and promote the occurrence of liver cancer. Ciprofloxacin, an effective broad-spectrum antimicrobial agent, can promote cell apoptosis and regulate the function of immune cells. As an important part of the tumor microenvironment, macrophages play an important role in tumor regulation. The present study demonstrated that the treatment of macrophages with ciprofloxacin was able to promote the production of interleukin-1β, tumor necrosis factor-α and the polarization of CD86⁺CD206⁻ macrophages, while inhibiting the polarization of CD86⁻CD206⁺ macrophages. This transformation may help macrophages promote tumor cell apoptosis, inhibit tumor cell proliferation, reduce metastasis and downregulate the phosphoinositide 3-kinase/AKT signaling pathway in liver cancer cell lines. *In vivo* experiments demonstrated that macrophages treated with ciprofloxacin inhibited the growth of subcutaneous implanted tumors in nude mice. In conclusion, the findings of the present study indicated that ciprofloxacin may inhibit liver cancer by upregulating the expression of CD86⁺CD206⁻ macrophages. This study further revealed the biological mechanism underlying the potential value of ciprofloxacin in antitumor therapy and provided new targets for the treatment of liver cancer.

Introduction

Liver cancer is one of the most common malignant tumors worldwide (1), and may be treated with several methods, such as surgery (2), radiotherapy (3) and chemotherapy (4). However, a number of patients miss the opportunity of potentially curative surgical treatment, as the early symptoms of primary liver cancer are not obvious (5) to enable early diagnosis. The application of radiotherapy and chemotherapy is also limited due to their toxicity and side effects. Therefore, it is crucial to explore the mechanism underlying the occurrence and development of liver cancer and identify novel treatment options.

With the increasing research interest in gut microbiota, the association between gut microbiota and tumors has been gradually elucidated (6,7). The liver and the gut are connected through the portal vein; therefore, the liver is not only perfused by abundant blood coming from the intestine, but is also affected by the gut microbiota, which may cause chronic inflammation of the liver tissue and increase the risk of liver cancer (8). It was reported that imbalance of gut microbiota may cause liver tissue damage and cirrhosis, thereby promoting the occurrence of liver cancer (9). It was also observed that the bacterial metabolite lipopolysaccharide (LPS) promoted liver tissue inflammation by binding to toll-like receptor (TLR)4, which increases the risk of liver cirrhosis and liver cancer (10). The inflammation of liver tissue also inhibited the function of CD8⁺ T cells and promoted liver cancer by promoting the aggregation of IgA⁺ (11). Referring to antibiotics as the major class of antibacterial agents, some studies explored their potential in antitumor therapy, and it was reported that bacterial depletion (vancomycin + neomycin + metronidazole + amphotericin) may inhibit the development of pancreatic cancer by restoring the function of CD8⁺ T cells and promoting the polarization and infiltration of M1-like macrophages (7).

It was also reported that bacterial depletion may inhibit the activation of TLR4 to reduce the incidence of liver cancer (9).

Ciprofloxacin, as a quinolone antibiotic, can be widely used in the treatment of the gastrointestinal tract by interacting with the topoisomerase II-DNA complexes and inhibiting the helix rejoining, thereby forming double-stranded DNA breaks and leading to bacterial death (12). In addition, ciprofloxacin exerts a certain effect against the eukaryotic topoisomerase IIα, a DNA gyrase analogue (13). Therefore, it was suggested that ciprofloxacin may inhibit the development of colorectal, pancreatic and breast cancer (14-16), among others, through its cytotoxic action, indicating its potential value in the treatment of tumors.

However, the occurrence and development of tumors is a complicated process. In addition to focusing on tumor cells, the role of the tumor microenvironment must not be overlooked (17,18). It has been demonstrated that the tumor microenvironment may be implicated in the poor efficacy of tumor treatment and drug resistance (19,20).

Tumor-associated macrophages (TAMs) are an important component of the tumor microenvironment. It was demonstrated that CD206⁻CD86⁺-M1-like macrophages could inhibit tumor development by enhancing antigen presentation, increasing the release of pro-inflammatory factors and promoting phagocytosis (21,22). Although it has been reported that the use of antibiotics in tumor therapy may promote the conversion of macrophages to M1-like TAMs (7), the effect of ciprofloxacin on macrophages remains controversial. Some studies reported that ciprofloxacin could inhibit the release of pro-inflammatory factors from macrophages induced by LPS (23), whereas other studies demonstrated that ciprofloxacin could promote macrophages to release tumor necrosis factor (TNF)-α in a non-bacterial-induced model (24). Therefore, in the present study, in order to further explore the association between ciprofloxacin, macrophages and liver cancer, the macrophages were treated with different concentrations of ciprofloxacin, the expression of the M1-like macrophage marker CD86 and the M2-like macrophage marker CD206 was detected, and then the effects of ciprofloxacin-induced macrophages (MCIP) on tumor cell proliferation, apoptosis and metastasis of liver cancer were investigated *in vitro* and *in vivo*.

Materials and methods

Specimens and patient data. A total of 30 liver cancer specimens were collected from the Pathology Archive of the First Affiliated Hospital of Chongqing Medical University (Chongqing, China) between January 2018 and January 2019, and these 30 liver cancer specimens were used to detect CD206 expression level by immunohistochemistry. The protocol of the present study was approved by the Medical Research Ethics Committee of Chongqing Medical University, and informed consent was obtained from all the patients.

Immunohistochemical staining. Paraffin sections (7 μm) of tumor tissues were dewaxed at room temperature, rehydrated and heat-treated for antigen retrieval with citric acid buffer at 98˚C for 20 min. The sections were then blocked with normal goat serum (C-0005, Bioss) for 30 min, incubated with primary antibody (CD206 1:3,000, cat. no. ab252921, Abcam) at 4˚C overnight, and were analyzed using an immunohistochemistry kit (PV-9001, ZSGB-BIO) following standardized protocol. The sections were counterstained with hematoxylin, mounted, and coverslipped. Staining intensity (cytoplasm and membrane) was independently assessed and defined as follows: 0, negative; 1, weak; 2, moderate; and 3, strong. The percentage of positive cells was defined as follows: 0, negative; 1, 1-20%; 2, 21-50%; and 3, 51-100%. The immunohistochemical staining score was calculated as staining intensity x percentage of positive cells and was defined as follows: 0, negative; 1-4, low; and >4, high.

Cell culture. Human liver cancer Huh7 and HepG2 cell lines were cultured in RPMI-1640 medium (HyClone; GE Healthcare Life Sciences) supplemented with 10% fetal bovine serum (FBS; Gibco; Thermo Fisher Scientific, Inc.) and 10 U/ml penicillin-streptomycin at 37˚C in a 5% CO_2 incubator. When the density of Huh7 and HepG2 cells reached 70-80%, the cells were processed with 0.5% trypsin and transferred to new dishes. The human monocyte THP-1 cell line was cultured in RPMI-1640 medium (HyClone; GE Healthcare Life Sciences) supplemented with 10% FBS at 37˚C in a 5% CO_2 incubator. A total of 100 ng/ml phorbol-12-myristate-13-acetate (PMA, Sigma-Aldrich; Merck KGaA, cat. no. P1585) was added to the culture medium to induce the transformation of $5x10^6$ monocytes into macrophages (M0) for 24 h. LPS (4 μg/ml; Sigma-Aldrich; Merck KGaA, cat. no. L4391) was added in the culture medium to induce the conversion of M0 into classical (M1-like) macrophages for 48 h. Interleukin (IL)-4 (100 ng/ml) and IL-10 (100 ng/ml) were added in the culture medium to induce the conversion of M0 into non-classical (M2-like) macrophages for 48 h. Various concentrations of ciprofloxacin (0.5, 1, 2.5, 5 and 10 μg/ml) were added in the culture medium to induce the conversion of M0 into ciprofloxacin-induced (MCIP) macrophages; subsequently, the precipitate was removed by centrifugation at 1,000 x g for 10 min at room temperature, and the clear supernatant extract of M0 and MCIP macrophages at 6, 12 and 24 h was collected to make a conditioned medium.

Western blotting. For the western blot analyses, RIPA buffer containing protease inhibitors and phosphatase inhibitors (Roche Diagnostics) was used to prepare whole-cell lysates. Protein (20 μg) from the lysates was separated by 10% SDS-PAGE and transferred to a PVDF membrane (0.45 μm, EMD Millipore). The membrane was blocked in 5% BSA (cat. no. A8020, Solarbio Life Science) at 37˚C for 2 h. After overnight incubation at 4˚C with primary antibodies (CD206 1:1,000, cat. no. ab252921, Abcam; Bcl2 1:1,000, cat. no. 15071, Cell Signaling Technology, Inc.; Bax 1:1,000, cat. no. 2774, Cell Signaling Technology, Inc.; p-AKT 1:1,000, cat. no. 4060, Cell Signaling Technology, Inc.; AKT 1:1,000, cat. no. 4685, Cell Signaling Technology, Inc.; CD86 1:1,000, YM0137, Immunoway; and β-actin 1:1,000, TA-09, ZSGB-BIO), the membranes were washed 3 times with 0.1% TBST (5 min per wash). After incubating with horseradish peroxidase-conjugated anti-mouse/rabbit IgG (1:3,000, cat. no. ZDR-5307/5306, ZSGB-BIO) at 37˚C for 1 h, the membranes were examined by enhanced chemiluminescence (cat. no. P0018AS, Beyotime Institute of Biotechnology).

RT-quantitative-PCR (RT-qPCR) analysis. Total RNA was extracted from Huh7 or HepG2 cells by TRIzol (TaKaRa Bio) and PrimeScriptTM RT Master Mix transcription kit (TaKaRa Bio) was used to reverse-trasncribe RNA into cDNA. The reverse transcription conditions were as follows: i) 37°C for 15 min; ii) 85°C for 5 sec. qPCR was performed in a CFX-connect fast real-time PCR system (Bio-Rad Laboratories, Inc.). The sample mixture was composed of 5 μl SYBR (TaKaRa Bio), 0.8 μl primers, 1 μl cDNA, and 3.2 μl ddH$_2$O. The thermocycling conditions were as follows: i) 95°C for 10 min; ii) 95°C for 20 sec; iii) 56°C for 10 sec; iv) the temperature was reduced by 3°C/cycle and steps ii-iv were repeated for 35 cycles; v) 95°C for 20 sec; and vi) 55°C for 20 sec.

The sequences of the primers used were as follows: TNF-α: Forward, 5'-GCCAACGGCATGGATCTCAA-3' and reverse, 5'-CAGCCTTGTCCCTTGAAGAGAAC-3'; IL-1β: Forward, 5'-GAAATGATGGCTTATTACAGTGGC-3' and reverse, 5'-TAGTGGTGGTCGGAGATTCGTAG-3'.

MTT. Huh7 and HepG2 cells (2×10^3/well) were inoculated into a 6-well plate and maintained in an incubator at 37°C with 5% CO$_2$ for ≤4 days. Cells in each well were treated with 10 μl MTT (5 mg/ml) for 4 h at 37°C. The medium was removed, and cells were lysed with 200 μl DMSO for 30 min. Cell viability was measured at 492 nm using an ELISA plate reader (BioTek Instruments, Inc.).

Crystal violet staining. Huh7 and HepG2 cells (3×10^4/well) were inoculated into a 24-well plate and the conditioned medium was added in each well for 48 h. The medium was removed and 500 μl 4% paraformaldehyde was added in each well at room temperature for 30 min, then cells were dyed by 500 μl 1% crystal violet solution at room temperature for 30 min. The cells were lysed with 200 μl glacial acetic acid and measured at 592 nm using an ELISA plate reader (BioTek Instruments, Inc.).

Hoechst staining. Huh7 and HepG2 cells (5×10^4/well) were inoculated into a 6-well plate, and treated with conditioned medium for 48 h, fixed with 4% paraformaldehyde and stained with 10 ng/ml Hoechst 33258 solution (Solarbio, cat. no. C0021). Increased condensation of chromatin was observed in apoptotic cells. Apoptotic cells were captured with an inverted fluorescence microscope (Nikon 80i; Nikon Corporation) in 3 random fields per experiment (magnification, x100).

Wound healing test. When the cell density reached >80% in the 6-well plate, conditioned medium with 1% FBS of M0 or MCIP was added in the 6-well plate. The cells were scratched with a small 10-μl pipette tip and washed with PBS 3 times (30 sec/per wash) before being observed and photographed under a microscope (Nikon 80i) at 0 and 24 h (magnification, x100). Then, the wound width was recorded at the same observation point. The mean wound width of multiple observation points was calculated, and the wound healing rate of each group was obtained.

Transwell assay. Transwell inserts (24-well, with an 8.0-μm pore polycarbonate membrane) were purchased from Corning, Inc. (cat. no. 3422). Matrigel (50 μl; cat. no. 356234, Corning,

Inc.) was used in the invasion experiment; the volume ratio of Matrigel and culture medium was 1:5. M0 or MCIP conditioned medium (400 μl) with 10% FBS containing 40,000 Huh7 cells or 40,000 HepG2 cells was added to each upper chamber, and 700 μl RPMI-1640 medium containing 15% FBS was added to the lower chamber. Four parallel controls were set up in each group. After 24 h, the cells on the lower side of the chamber membrane were fixed for 20 min with 500 μl 4% paraformaldehyde at room temperature. The cells were stained with 500 μl 1% crystal violet solution for 30 min at room temperature. After washing and drying, the cells were counted under a microscope (Nikon 80i) at a magnification of x100. At least 10 visual fields were observed in each chamber, and the mean values were obtained after counting.

In vivo experiment. A total of 14 specific pathogen-free male BALB/c nude mice, aged 6 weeks and weighing 20±1 g, were purchased from HFK Bioscience Co. Ltd. The nude mice were randomly divided into two groups (Huh7 group, n=5; Huh7 + MCIP group, n=9). Huh7 cells (5×10^6) with or without MCIP (1×10^7) were suspended in 100 μl PBS, and then inoculated into the subcutaneous region of the right upper armpit of the nude mice. The tumors were resected 3 weeks after implantation. The length (a) and width (b) of each tumor were measured, and the tumor volume (V) was calculated as follows: $V = a \times b^2 \times \pi/6$. The experimental procedures, which ensured the safety of practitioners in laboratory animal projects and conformed to ethical standards and international practices, were approved by the Animal Experimental Ethics Committee of Chongqing Medical University. The animals were fed a standard laboratory diet with free access to food and water, and were kept in a room at controlled temperature (22±1°C) and humidity (65-70%), with a 12-h light-dark cycle. After the study, all animals were anaesthetized by isoflurane inhalation (1.5-2%) and then euthanized by cervical dislocation. All animal experiments conformed to the guidelines from Directive 2010/63/EU of the European Parliament on the protection of animals used for scientific purposes.

Statistical analysis. SPSS 16.0 statistical software (SPSS, Inc.) was used to analyze the experimental results. Each experiment was repeated three times. The differences between groups were evaluated by t-test or Bonferroni-corrected t-test. $P < 0.05$ was considered to indicate statistically significant differences.

Results

Ciprofloxacin promotes CD86⁺CD206⁻ macrophage polarization. Among macrophages, which are an important component of the tumor microenvironment, non-classical (M2-like) macrophages can promote tumors, while classical (M1-like) macrophages can inhibit tumors. In accordance with existing reports, the immunohistochemistry examination demonstrated that the expression of CD206, a marker of M2-like macrophages, was higher in the low-differentiation group compared with that in the high-differentiation group (Fig. 1A).

To investigate the association between ciprofloxacin and macrophage polarization, M0 macrophages were exposed to ciprofloxacin (MCIP) at various concentrations. The western blot analysis revealed that the M1-like macrophage-related
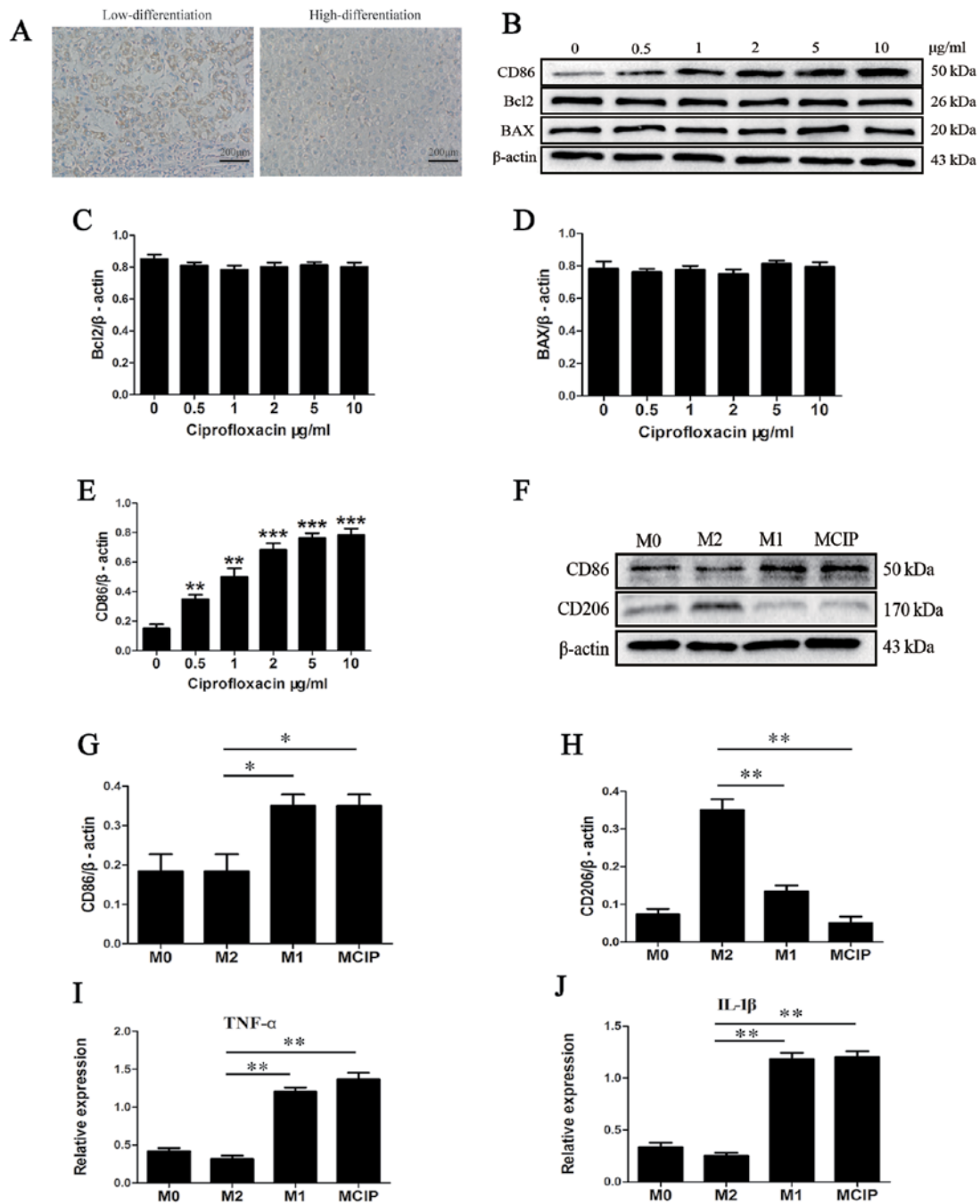
Figure 1. Ciprofloxacin promotes CD86⁺CD206⁻ macrophage polarization. (A) The expression of CD206 in highly and poorly differentiated liver cancer tissues by immunohistochemistry (low differentiation, n=15; high differentiation, n=15). (B) The protein levels of CD86, Bcl2 and BAX were detected by western blotting in macrophages after treatment with different concentrations of ciprofloxacin. Densitometry analysis was used to quantify the expression of (C) Bcl2, (D) BAX and (E) CD86 (*P<0.05 **P<0.005 ***P<0.001 vs. 0 μg/ml group). (F) The protein levels of CD86 and CD206 were detected by western blotting in M0 macrophages (M0), M1-like macrophages (M1), M2-like macrophages (M2) and ciprofloxacin-induced macrophages (MCIP). Densitometry analysis was used to quantify the expression of (G) CD86 (*P<0.05 vs. M2 group) and (H) CD206 (**P<0.005 vs. M2 group). (I) The mRNA level of TNF-α was detected by quantitative PCR in the M0, M1, M2 and MCIP groups (**P<0.005 vs. M2 group). (J) The mRNA level of IL-1β was detected by quantitative PCR in the M0, M1, M2 and MCIP groups (**P<0.005 vs. M2 group). TNF tumor necrosis factor; IL, interleukin.

marker CD86 was upregulated (Fig. 1B and E), while the protein levels of Bcl2 and BAX were not affected by ciprofloxacin (Fig. 1B-D); accordingly, in the subsequent experiments, 2 μg/ml ciprofloxacin was used to treat macrophages. When using M1-like and M2-like macrophages as a reference, it was observed that CD86 was upregulated in M0 by ciprofloxacin treatment; by contrast, the M2-like macrophage-related marker CD206 was downregulated (Fig. 1F-H). Subsequently, the

expression of cytokines was investigated and it was observed that the pro-inflammatory factors TNF-α and IL-1β were upregulated in M1-like and MCIP macrophages (Fig. 1I and J); by contrast, these cytokines were downregulated in M2-like macrophages.

Effect of MCIP on the proliferation and apoptosis of liver cancer cells. It was observed in previous experiments that ciprofloxacin
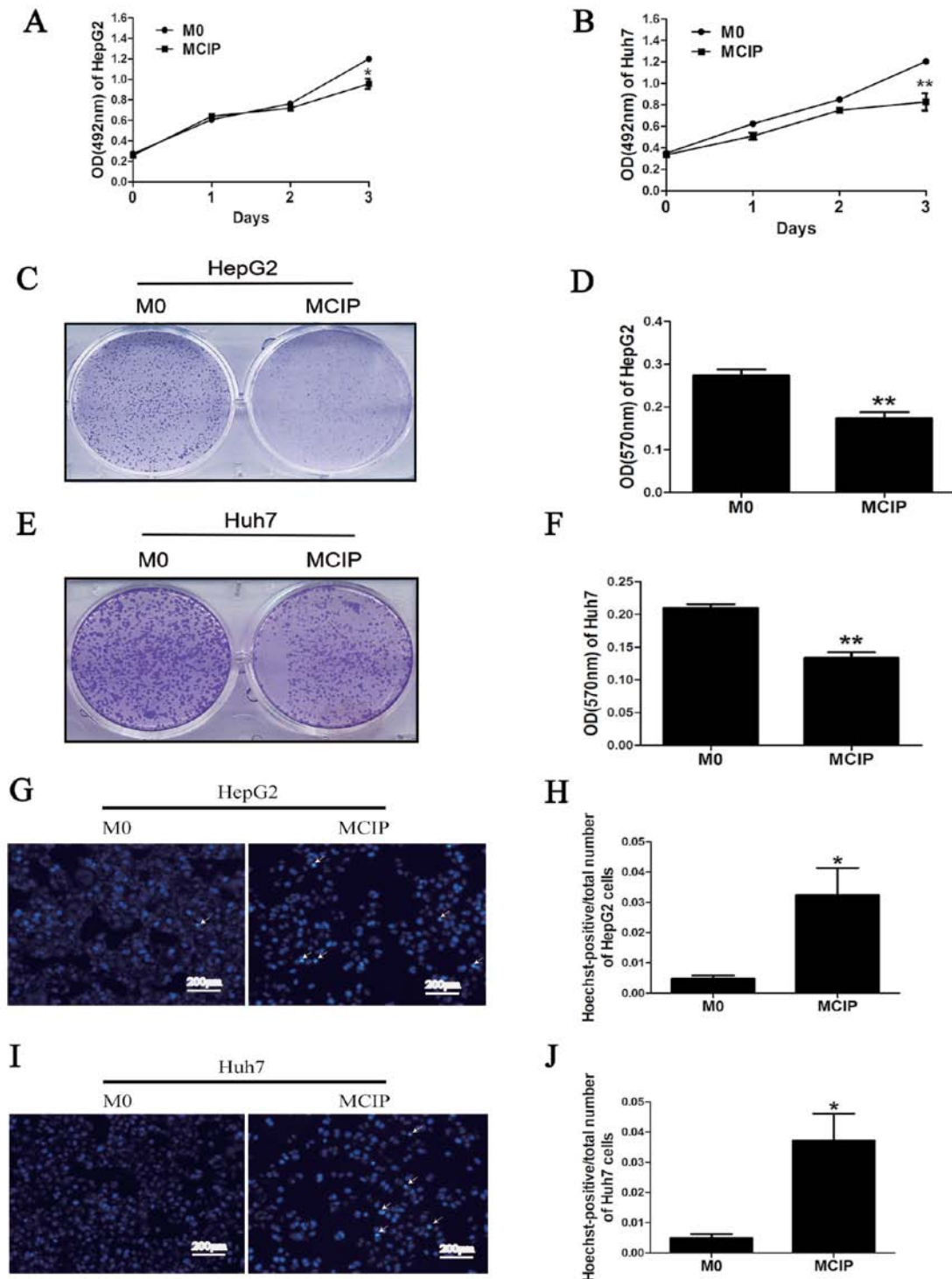
Figure 2. Effect of MCIP on the proliferation and apoptosis of liver cancer cells. (A) The proliferation ability of HepG2 cells after treatment with conditioned medium from M0 or MCIP macrophages was detected by MTT assay ($^*P<0.05$ vs. M0 group). (B) The proliferation ability of Huh7 cells after treatment with conditioned medium from M0 or MCIP macrophages was detected by MTT assay ($^{**}P<0.005$ vs. M0 group). (C) The number of HepG2 cells after treatment with conditioned medium was detected by crystal violet staining. (D) Quantitative result of crystal violet staining of HepG2 cells ($^{**}P<0.005$ vs. M0 group). (E) The number of Huh7 cells after treatment with conditioned medium was detected by crystal violet staining. (F) Quantitative result of crystal violet staining of Huh7 cells ($^{**}P<0.005$ vs. M0 group). (G) The apoptosis of HepG2 cells after treatment with conditioned medium was detected by Hoechst staining. (H) The number of HepG2 cells was measured ($^{**}P<0.005$ vs. M0 group). (I) The apoptosis ability of Huh7 was detected by Hoechst staining. (J) The number of HepG2 cells was measured ($^{**}P<0.005$ vs. M0 group). MCIP, ciprofloxacin-induced macrophages.

increased the number of CD86$^+$CD206$^-$ macrophages, but it was uncertain whether this group of macrophages exerted a tumor-suppressive effect similar to that of M1-like macrophages; therefore, the following experiment was conducted: The conditioned medium of MCIP was collected to treat HepG2 and

Huh7 cells. MTT assay demonstrated that the OD values did not differ significantly between the groups on days 0, 1 and 2. However, on day 3, the OD values of HepG2 (Fig. 2A) and Huh7 (Fig. 2B) cells in the MCIP conditioned medium group were significantly lower compared with those in the control group.
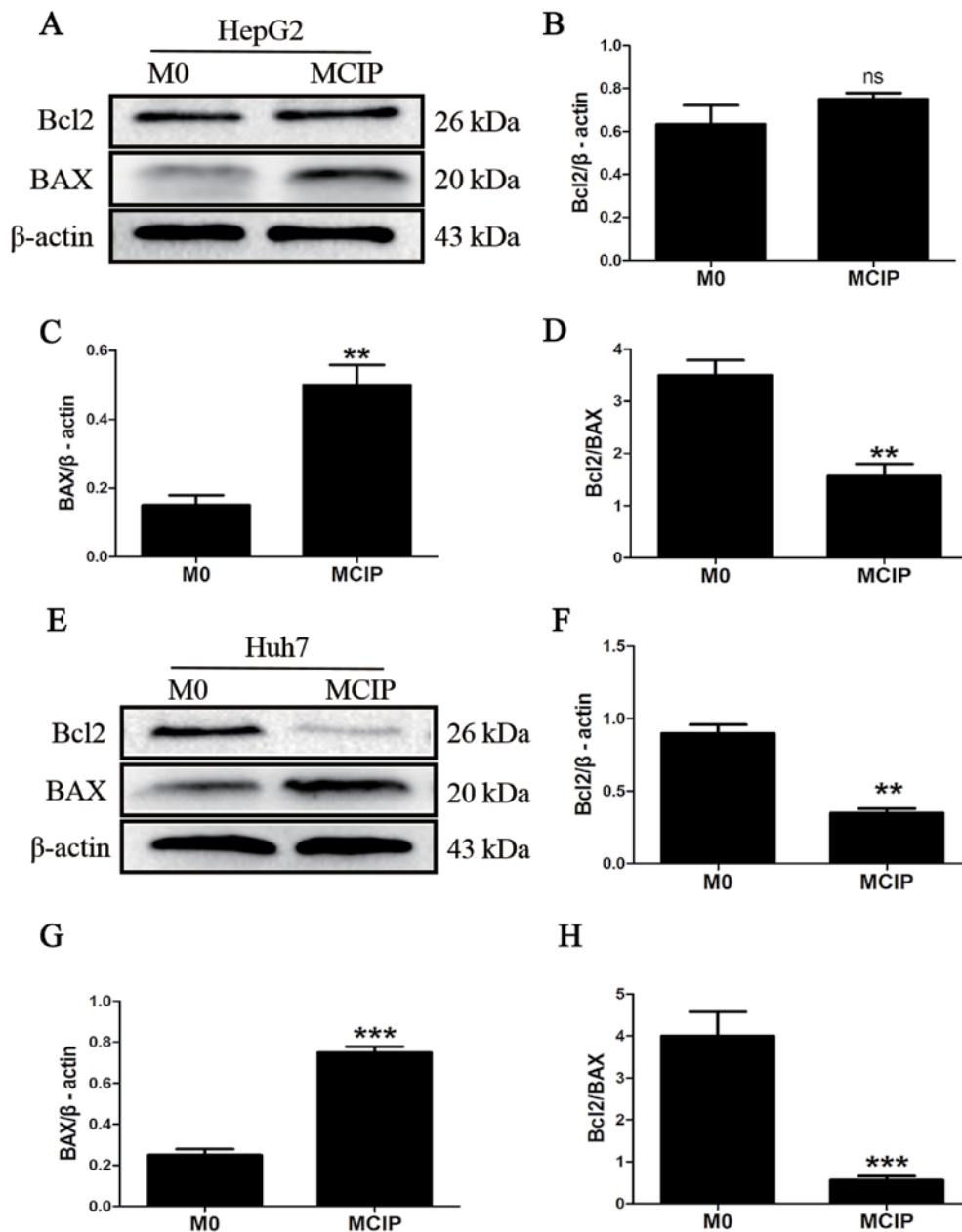
Figure 3. Effect of MCIP on apoptosis of liver cancer cells. (A) The protein levels of Bcl2 and BAX of HepG2 cells after treatment with conditioned medium from M0 or MCIP macrophages were detected by western blotting. Densitometry analysis was used to quantify the expression of (B) Bcl2, (C) BAX and (D) Bcl2/BAX (**P<0.005 vs. M0 group). (E) The protein levels of Bcl2 and BAX in Huh7 cells after treatment with conditioned medium were detected by western blotting. Densitometry analysis quantify the expression of (F) Bcl2, (G) BAX and (H) Bcl2/BAX (**P<0.005 vs. M0 group; ***P<0.001 vs. M0 group). MCIP, ciprofloxacin-induced macrophages; ns, not significant.

The results of crystal violet staining revealed that the number of HepG2 (Fig. 2C and D) and Huh7 (Fig. 2E and F) cells was lower in the MCIP group compared with the M0 group. These results demonstrated that macrophages inhibited the proliferation of liver cancer cells to a greater extent following ciprofloxacin treatment. To investigate the effect of MCIP on the apoptosis of liver cancer cells, Hoechst staining was used, and it demonstrated typical apoptotic changes of the nuclei of HepG2 (Fig. 2G and H) and Huh7 (Fig. 2I and J) cells in the MCIP conditioned medium group, and that the numbers of HepG2 and Huh7 cells in the MCIP conditioned medium group were lower compared with those in the control group. To compare with the results of previous studies, it was reported that the protein levels

of Bcl2 were downregulated in Huh7 cells (Fig. 3E and F) and were unaffected in HepG2 cells (Fig. 3A and B), while BAX was upregulated in Huh7 (Fig. 3E and G) and HepG2 (Fig. 3A and C) cells. However, the Bcl2/BAX ratio was decreased in HepG2 (Fig. 3D) and Huh7 (Fig. 3H) cells following treatment with MCIP conditioned medium.

Effect of MCIP on the migration and invasion of liver cancer cells. To explore the role of MCIP in metastasis, the wound healing test was used. It revealed that the migration abilities of HepG2 (Fig. 4I and J) and Huh7 (Fig. 4K and L) cells were inhibited by treatment with MCIP conditioned medium. To verify the effect of MCIP on the migration abilities of HepG2

and Huh7 cells, Transwell assays without Matrigel revealed that the transmembrane numbers of HepG2 (Fig. 4A and B) and Huh7 (Fig. 4C and D) cells were lower in the MCIP conditioned group compared with those in the control group. The Transwell assay with Matrigel was used to verify the effect of MCIP on the invasion abilities of HepG2 (Fig. 4E and F) and Huh7 (Fig. 4G and H). The results revealed that the transmembrane numbers of Huh7 and HepG2 cells were lower in the MCIP conditioned group compared with those in the control group.

Effect of the phosphatidylinositol 3-kinase (PI3K)/AKT signaling pathway on the regulation of liver cancer cells by MCIP. PI3K/AKT has been proven to play a key role in the pathogenic process of tumors. To verify whether this signaling pathway was involved in regulating liver cancer, western blotting was used. The results revealed that the level of phosphorylated AKT (p-AKT) was downregulated in HepG2 (Fig. 5A) and Huh7 (Fig. 5C) cells by adding MCIP conditioned medium compared with the control group, whereas the total AKT level did not differ between the MCIP conditioned medium and control groups (Fig. 5A and C). Therefore, the p-AKT/AKT ratio was decreased in HepG2 (Fig. 5B) and Huh7 (Fig. 5D) cells after treatment with MCIP conditioned medium.

Effect of MCIP on Huh7 cells in vivo. To demonstrate the effect of MCIP on liver cancer cells *in vivo*, the subcutaneous tumorigenicity test was used. Huh7 cells were used, as the tumorigenesis rate of Huh7 cells was higher compared with that of HepG2 cells. Huh7 cells ($5x10^6$) were injected into the armpit of nude mice together with $1x10^7$ ciprofloxacin-treated macrophages (MCIP) to construct a subcutaneous tumor model. As expected, the tumor size of the Huh7 + MCIP group was smaller compared with that of the Huh7 group (Fig. 5E and F). The results of the *in vivo* experiments were consistent with those of the *in vitro* experiments.

Discussion

Liver cancer is one of the most common malignant tumors worldwide. The annual death toll of patients with liver cancer is reported to be as high as 745,000. The occurrence and development of liver cancer is a complex process involving multiple factors. Due to the insidious symptoms at the early stages of liver cancer, the majority of the patients miss the opportunity for surgical treatment. Moreover, the efficacy of other conventional treatments, such as chemotherapy, radiotherapy and molecular targeted drugs, has also been limited in clinical application due to the associated toxic side effects and drug resistance (25-28). Consequently, the development of preventive or therapeutic strategies adopting novel mechanisms, such as the application of antibiotics targeting liver cancer-related immunity mechanisms, is imminent.

Ciprofloxacin belongs to the class of quinolone antibiotics (29). Its main mechanism of antibacterial activity is to inhibit bacterial DNA replication and division by acting on the topoisomerase II and topoisomerase IV of bacteria. However, mammalian topoisomerase II is also one of the targets of certain antitumor drugs (30). Due to the similarities in the

DNA synthesis mechanism for topoisomerase II between mammals and bacteria, quinolone antibiotics have also been investigated in the field of antitumor research. It was demonstrated that ciprofloxacin could induce apoptosis of tumor cells through its cytotoxic action (14-16).

Although numerous studies have investigated the direct effects of ciprofloxacin on tumors, there are only few studies on the effects of ciprofloxacin on the components of the tumor microenvironment, such as TAMs. In the present study, it was observed that ciprofloxacin at 0.5, 1, 2.5, 5 and 10 μg/ml promoted the expression of CD86, which was highly expressed in M1-like TAMs (31,32), while the expressions of IL-1β and TNF-α were also increased; conversely, the expression of the CD206, which was highly expressed in M2-like TAMs (33-35), was reduced. TAMs are a complex group, and each member exhibits various biological characteristics and functions. Some studies confirmed that M1-like TAMs had strong phagocytic and antigen-presenting abilities, and secreted a large number of pro-inflammatory factors, which contributed to bacterial elimination and antitumor immunity (36,37); on the contrary, M2-like TAMs exhibited reduced phagocytic and antigen-presenting abilities, and could secrete anti-inflammatory factors to suppress the immune response and promote tumor progression (33,38,39). It was observed herein that ciprofloxacin promoted the expression of CD86 and inhibited the expression of CD206. This result suggested that ciprofloxacin may be involved in the regulation of M0 TAMs to CD86+CD206--M1-like macrophages. Accordingly, in order to elucidate whether the macrophages treated with ciprofloxacin promote tumor inhibition, in-depth investigation and analysis were conducted in this study.

Due to the regulatory interaction between tumor cells and TAMs (40), in order to avoid the interference of tumor cells in MCIP, the method of co-culture was excluded, and MCIP conditioned medium was prepared to verify the MCIP function. It was demonstrated that the MCIP conditioned medium could inhibit the proliferation of liver cancer cells by MTT assay, while crystal violet staining, Hoechst staining and the Bcl2/BAX ratio demonstrated that the addition of MCIP conditioned medium could reduce the number of liver cancer cells and promote cell apoptosis. In addition, the caspase pathway and the presence of phosphatidylserine on the exterior surface of the plasma membrane may also be used to verify the effect of ciprofloxacin on cell apoptosis; therefore, the mechanism through which MCIP conditioned medium regulates apoptosis of liver cancer cells required further investigation. Transwell and wound healing experiments revealed that the addition of MCIP conditioned medium inhibited the migration and invasion of liver cancer cells, and downregulated the level of p-AKT. It was also observed *in vivo* that the subcutaneous tumors of nude mice that had received MCIP treatment were smaller. In summary, MCIP conditioned medium inhibited the proliferation, migration and invasion of liver cancer cells, as well as subcutaneous tumor formation, and promoted apoptosis. However, due to the limitation of conditioned medium preparation in this study, conditioned medium containing 1% FBS was used for the wound healing experiments. Therefore, in order to exclude the interference of proliferation, in addition to the Transwell assay, more experiments are required to verify the effect of MCIP on the migration and invasion of liver cancer cells. Furthermore, the composition of the conditioned medium is complicated,
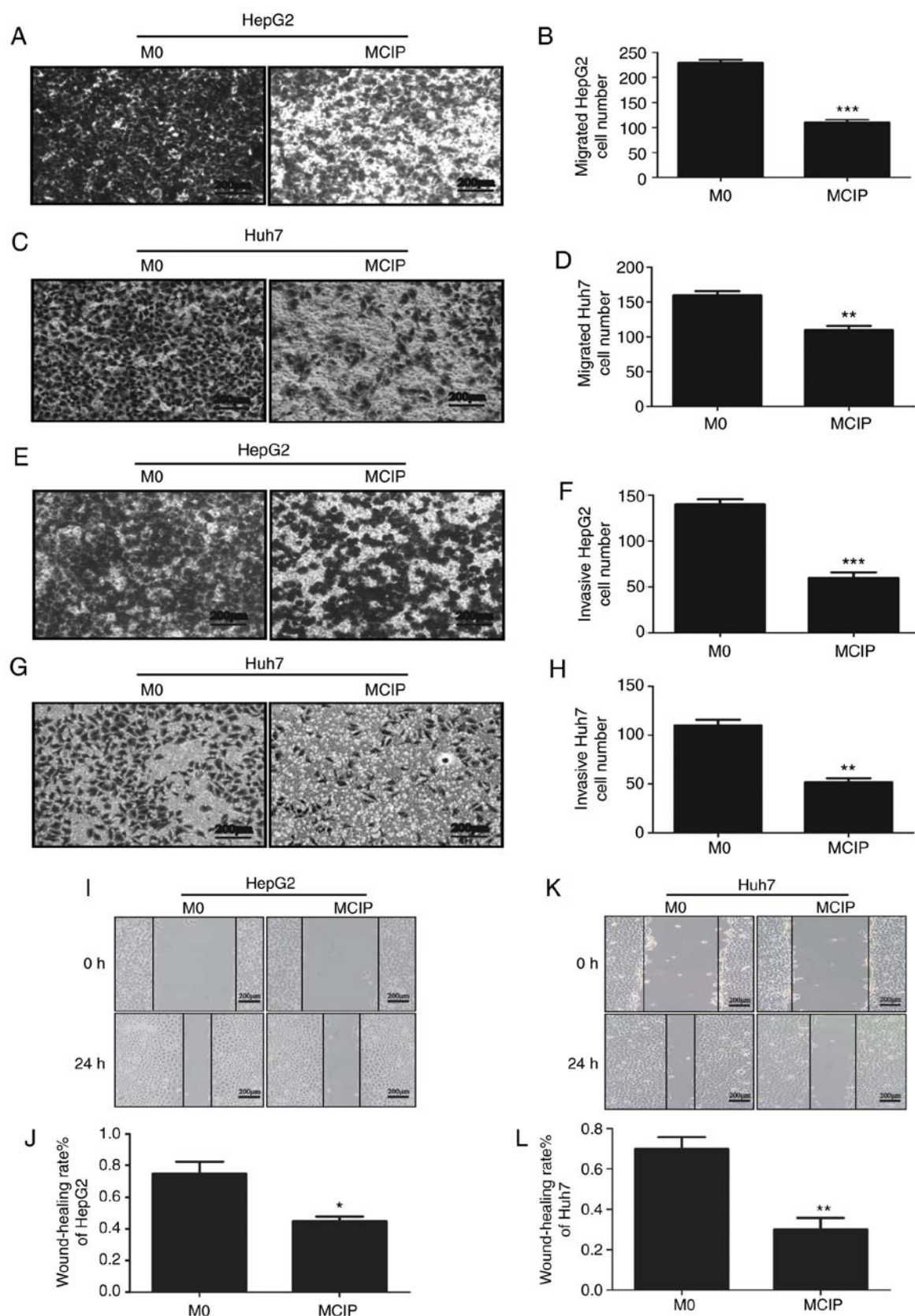
Figure 4. Effect of MCIP on migration and invasion of liver cancer cells. (A and B) The migration ability of HepG2 cells was analyzed by Transwell assay without Matrigel after treatment with conditioned medium from M0 or MCIP macrophages (***P<0.001 vs. M0 group). (C and D) The migration ability of Huh7 cells was analyzed by Transwell assay without Matrigel after treatment with conditioned medium from M0 or MCIP macrophages (**P<0.005 vs. M0 group). (E and F) The migration ability of HepG2 cells was analyzed by Transwell assay with Matrigel after treatment with conditioned medium from M0 or MCIP macrophages (***P<0.001 vs. M0 group). (G and H) The migration ability of Huh7 cells was analyzed by Transwell assay with Matrigel after treatment with conditioned medium from M0 or MCIP macrophages (***P<0.001 vs. M0 group). (I and J) The metastatic ability of HepG2 cells after treatment with conditioned medium from M0 or MCIP macrophages was examined by wound healing test (*P<0.05 vs. M0 group). (K and L) The metastasis ability of Huh7 cells after treatment with conditioned medium from M0 or MCIP macrophages was performed by wound healing test (**P<0.005 vs. M0 group). MCIP, ciprofloxacin-induced macrophages.
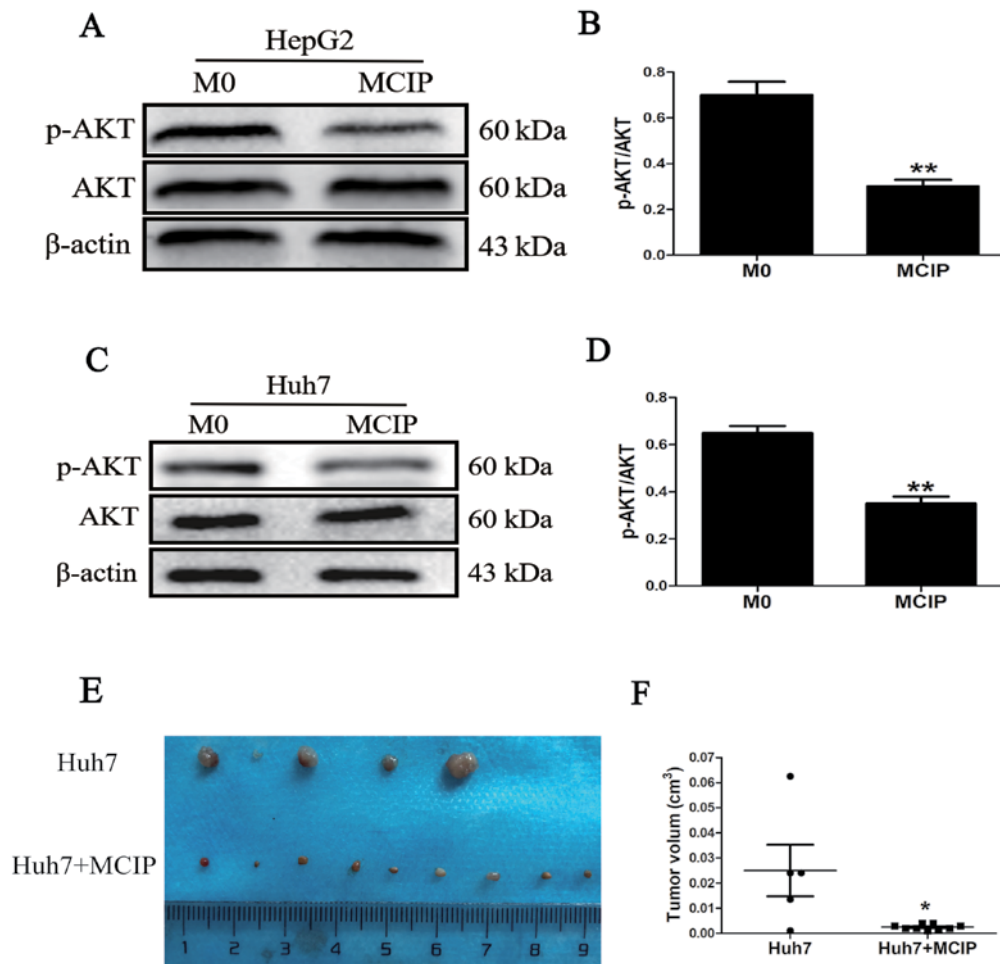
Figure 5. Effect of the PI3K/AKT signaling pathway on the regulation of liver cancer cells by MCIP and the effect of MCIP on liver cancer cells *in vivo*. (A) The protein levels of p-AKT and AKT in HepG2 cells after treatment with conditioned medium from M0 or MCIP macrophages were detected by western blotting. (B) Densitometry analysis was used to quantify the expression of p-AKT/AKT (**P<0.005 vs. M0 group). (C) The protein levels of p-AKT and AKT in Huh7 cells after treatment with conditioned medium from M0 or MCIP macrophages were detected by western blotting. (D) Densitometry analysis was used to quantify the expression of p-AKT/AKT (**P<0.005 vs. M0 group). (E) The Huh7 tumors were resected from nude mice 3 weeks after tumor implantation (Huh7 group, n=5; Huh7 + MCIP group, n=9). (F) Statistical analysis of tumor volume (*P<0.05 vs. M0 group). PI3K, phosphatidylinositol 3-kinase; MCIP, ciprofloxacin-induced macrophages.

and the contributions made by specific cytokines towards the overall regulatory function require follow-up experiments to verify.

The occurrence and development of tumors is a complex process, and the effect of the tumor microenvironment is suggested to be significant, particularly in promoting tumors and inhibiting the effects of drug treatment (19,20). It was previously confirmed that M2-like TAMs promote tumor angiogenesis by secreting vascular endothelial growth factor (41), degrade extracellular matrix by inducing the secretion of matrix metallopeptidases, promote vascular endothelial cell migration and facilitate tumor cell metastasis (42,43). Therefore, the investigation of macrophages as a therapeutic target may be of considerable value in tumor immunotherapy. It was observed in the present study that ciprofloxacin could increase the number of CD86^{+}CD206^{-} macrophages and inhibit the progression of liver cancer, which further elucidated the mechanism and potential of ciprofloxacin in the treatment of liver cancer. The results revealed that ciprofloxacin-induced macrophages (MCIP) highly expressed CD86, TNF-α and IL-1β; however, in other experiments, it was confirmed that MCIP could regulate the proliferation,

metastasis and apoptosis of liver cancer, which was similar to the functions of M1-like TAMs. However, the classification of TAMs is complicated. In addition to the classical CD86 and CD206, CD163, CD204, CD200R and some cytokines may also be used for the identification of M1-like and M2-like macrophages (44,45). Although increased expression levels of CD86, TNF-α and IL-1β were observed, the decreased expression of CD206 in macrophages after treatment with ciprofloxacin and MCIP also exerted some tumor-inhibitory effects. However, other studies reported that ciprofloxacin could promote the expression of TNF-α and did not affect the expression of IL-1β in animal models (46). The changes in these cytokines were not consistent with the classical model of LPS-induced M1-like macrophage polarization (47). Thus, although MCIP overexpressed CD86 with low expression of CD206 and exhibited the similar tumor-suppressive trend as M1-like TAMs, the identification of macrophage types prone to MCIP requires more indicators for validation.

It was previously reported that ciprofloxacin could inhibit the secretion of TNF-α and IL-1β from microglia and other cells following stimulation by LPS (23), but other studies reported that ciprofloxacin could promote the expression of TNF-α and reduce

the expression of IL-10 (48), which suggested that ciprofloxacin played different roles in different disease models and different types of immune cells. In order to investigate the effect of ciprofloxacin on TAMs in our experiments, an experimental model of THP-1 monocytes transforming into macrophages was induced by the addition of PMA (49,50). Therefore, in the follow-up study, extraction of primary TAMs will be planned to explore the regulation on macrophage function by ciprofloxacin. In order to explore the effect of MCIP on tumor development, MCIP conditioned medium was adopted to observe the effect of MCIP on liver cancer cell proliferation, apoptosis, migration and invasion, while the effect on tumor occurrence resulting from the interaction between oncogenic cells and the microenvironment was investigated. Although it has been reported that tumor cells could regulate the transformation of TAMs to M2-like TAMs through various pathways, in our experiments, only the effects of MCIP on tumors were explored, whereas the possible regulatory effects of tumor cells on MCIP were not. Therefore, in the follow-up study, the experimental design should take into consideration both aspects of tumor cell-MCIP interactions, to further elucidate the association between ciprofloxacin, TAMs and liver cancer.

Although a number of studies confirmed that ciprofloxacin may be used to inhibit the development of a wide range of tumors, ciprofloxacin cannot differentiate between tumor cells and normal tissue, as it targets topoisomerases of all eukaryotes (51). While ciprofloxacin directly acts on tumor cells, it may also damage normal cells, inducing certain adverse reactions. In addition, drug resistance is also an unavoidable limitation of this antibiotic (52). It was observed in the experiment that ciprofloxacin-induced MCIP exerted a certain inhibitory effect on tumors, but similar to M1-like macrophages, their inhibitory effects on cells were not cell-specific. It was reported that M1-like macrophage overactivation may be associated with cardiovascular (53), autoimmune (54) and metabolic (55) diseases, so extensive investigation is still required before the clinical application of ciprofloxacin in antitumor therapy. More in-depth research is required to verify the effect of ciprofloxacin on macrophage polarization and to further explore its specific regulatory mechanisms.

In summary, the present study further elucidated the biological mechanism underlying the potential applicability of ciprofloxacin in antitumor therapy and indicated new potential targets for the treatment of liver cancer.

Acknowledgements

Availability of data and materials

The datasets generated during and/or analyzed during the present study are available from the corresponding author on reasonable request.

Authors' contributions

QS conceived and supervised the study. MTF obtained most data and wrote the manuscript. SCC was responsible for collating experimental data. YGW, MJB, LQA, JHW and MYZ were responsible for data analysis. XL provided the liver cancer specimens. YJJ, XWW and GGH designed the methods of the experiments. MHZ and BC were responsible for checking the manuscript. All authors participated in data interpretation. All the authors have read and approved the final version of the manuscript.

Ethics approval and consent to participate

The present study was approved by the Medical Research Ethics Committee of Chongqing Medical University, and written informed consent was obtained from all patients.

Patient consent for publication

Not applicable.

Competing interests

The authors declare that they have no competing interests.

References

1. Bray F, Ferlay J, Soerjomataram I, Siegel RL, Torre LA and Jemal A: Global cancer statistics 2018: GLOBOCAN estimates of incidence and mortality worldwide for 36 cancers in 185 countries. CA Cancer J Clin 68: 394-424, 2018.
2. Eggert T and Greten TF: Current standard and future perspectives in non-surgical therapy for hepatocellular carcinoma. Digestion 96: 1-4, 2017.
3. Ohri N, Dawson LA, Krishnan S, Seong J, Cheng JC, Sarin SK, Kinkhabwala M, Ahmed MM, Vikram B, Coleman CN and Guha C: Radiotherapy for hepatocellular carcinoma: New indications and directions for future study. J Natl Cancer Inst 108: djw133, 2016.
4. Ikeda M, Morizane C, Ueno M, Okusaka T, Ishii H and Furuse J: Chemotherapy for hepatocellular carcinoma: Current status and future perspectives. Jpn J Clin Oncol 48: 103-114, 2018.
5. Kim E, Lisby A, Ma C, Lo N, Ehmer U, Hayer KE, Furth EE and Viatour P: Promotion of growth factor signaling as a critical function of β-catenin during HCC progression. Nat Commun 10: 1909, 2019.
6. Geller LT, Barzily-Rokni M, Danino T, Jonas OH, Shental N, Nejman D, Gavert N, Zwang Y, Cooper ZA, Shee K, *et al*: Potential role of intratumor bacteria in mediating tumor resistance to the chemotherapeutic drug gemcitabine. Science 357: 1156-1160, 2017.
7. Pushalkar S, Hundeyin M, Daley D, Zambirinis CP, Kurz E, Mishra A, Mohan N, Aykut B, Usyk M, Torres LE, *et al*: The pancreatic cancer microbiome promotes oncogenesis by induction of innate and adaptive immune suppression. Cancer Discov 8: 403-416, 2018.
8. Zhang HL, Yu LX, Yang W, Tang L, Lin Y, Wu H, Zhai B, Tan YX, Shan L, Liu Q, *et al*: Profound impact of gut homeostasis on chemically-induced pro-tumorigenic inflammation and hepatocarcinogenesis in rats. J Hepatol 57: 803-812, 2012.
9. Yu LX and Schwabe RF. The gut microbiome and liver cancer: Mechanisms and clinical translation. Nat Rev Gastroenterol Hepatol 14: 527-539, 2017.

10. Dapito DH, Mencin A, Gwak GY, Pradere JP, Jang MK, Mederacke I, Caviglia JM, Khiabanian H, Adeyemi A, Bataller R, *et al*: Promotion of hepatocellular carcinoma by the intestinal microbiota and TLR4. Cancer Cell 21: 504-516, 2012.

11. Shalapour S, Lin XJ, Bastian IN, Brain J, Burt AD, Aksenov AA, Vrbanac AF, Li W, Perkins A, Matsutani T, *et al*: Inflammation-induced IgA+ cells dismantle anti-liver cancer immunity. Nature 551: 340-345, 2017.

12. Aldred KJ, Kerns RJ and Osheroff N: Mechanism of quinolone action and resistance. Biochemistry 53: 1565-1574, 2014.

13. Hangas A, Aasumets K, Kekalainen NJ, Paloheinä M, Pohjoismäki JL, Gerhold JM and Goffart S: Ciprofloxacin impairs mitochondrial DNA replication initiation through inhibition of Topoisomerase 2. Nucleic Acids Res 46: 9625-9636, 2018.

14. Herold C, Ocker M, Ganslmayer M, Gerauer H, Hahn EG and Schuppan D: Ciprofloxacin induces apoptosis and inhibits proliferation of human colorectal carcinoma cells. Br J Cancer 86: 443-448, 2002.

15. Beberok A, Wrzesniok D, Rok J, Rzepka Z, Respondek M and Buszman E: Ciprofloxacin triggers the apoptosis of human triple-negative breast cancer MDA-MB-231 cells via the p53/Bax/Bcl-2 signaling pathway. Int J Oncol.V 52: 1727-1737, 2018.

16. Yadav V, Varshney P, Sultana S, Yadav J and Saini N: Moxifloxacin and ciprofloxacin induces S-phase arrest and augments apoptotic effects of cisplatin in human pancreatic cancer cells via ERK activation. BMC Cancer 15: 581, 2015.

17. Bottcher JP, Bonavita E, Chakravarty P, Blees H, Cabeza-Cabrerizo M, Sammicheli S, Rogers NC, Sahai E, Zelenay S and Reis e Sousa C: NK cells stimulate recruitment of cDC1 into the tumor microenvironment promoting cancer immune control. Cell 172: 1022-1037 e14, 2018.

18. Su S, Chen J, Yao H, Liu J, Yu S, Lao L, Wang M, Luo M, Xing Y, Chen F, *et al*: CD10+GPR77+ cancer-associated fibroblasts promote cancer formation and chemoresistance by sustaining cancer stemness. Cell 172: 841-856 e16, 2018.

19. Huelsken J and Hanahan D: A subset of cancer-associated fibroblasts determines therapy resistance. Cell 172: 643-644, 2018.

20. Dalton HJ, Pradeep S, McGuire M, Hailemichael Y, Ma S, Lyons Y, Armaiz-Pena GN, Previs RA, Hansen JM, Rupaimoole R, *et al*: Macrophages facilitate resistance to anti-VEGF therapy by altered VEGFR expression. Clin Cancer Res 23: 7034-7046, 2017.

21. Chavez-Galan L, Olleros ML, Vesin D and Garcia I: Much more than M1 and M2 macrophages, there are also CD169(+) and TCR(+) macrophages. Front Immunol 6: 263, 2015.

22. Huang YK, Wang M, Sun Y, Di Costanzo N, Mitchell C, Achuthan A, Hamilton JA, Busuttil RA and Boussioutas A: Macrophage spatial heterogeneity in gastric cancer defined by multiplex immunohistochemistry. Nat Commun 10: 3928, 2019.

23. Zusso M, Lunardi V, Franceschini D, Pagetta A, Lo R, Stifani S, Frigo AC, Giusti P and Moro S: Ciprofloxacin and levofloxacin attenuate microglia inflammatory response via TLR4/NF-kb pathway. J Neuroinflammation 16: 148, 2019.

24. Shaki F, Ashari S and Ahangar N: Melatonin can attenuate ciprofloxacin induced nephrotoxicity: Involvement of nitric oxide and TNF-α. Biomed Pharmacother 84: 1172-1178, 2016.

25. Bray F, Ferlay J, Laversanne M, Brewster DH, Gombe Mbalawa C, Kohler B, Piñeros M, Steliarova-Foucher E, Swaminathan R, Antoni S, *et al*: Cancer incidence in five continents: Inclusion criteria, highlights from Volume X and the global status of cancer registration. Int J Cancer 137: 2060-2071, 2015.

26. Broutier L, Mastrogiovanni G, Verstegen MM, Francies HE, Gavarró LM, Bradshaw CR, Allen GE, Arnes-Benito R, Sidorova O, Gaspersz MP, *et al*: Human primary liver cancer-derived organoid cultures for disease modeling and drug screening. Nat Med 23: 1424-1435, 2017.

27. van Malenstein H, Dekervel J, Verslype C, Van Cutsem E, Windmolders P, Nevens F and van Pelt J: Long-term exposure to sorafenib of liver cancer cells induces resistance with epithelial-to-mesenchymal transition, increased invasion and risk of rebound growth. Cancer Lett 329: 74-83, 2013.

28. Yang JD, Hainaut P, Gores GJ, Amadou A, Plymoth A and Roberts LR: A global view of hepatocellular carcinoma: Trends, risk, prevention and management. Nat Rev Gastroenterol Hepatol 16: 589-604, 2019.

29. Zhang GF, Liu X, Zhang S, Pan B and Liu ML: Ciprofloxacin derivatives and their antibacterial activities. Eur J Med Chem 146: 599-612, 2018.

30. Delgado JL, Hsieh CM, Chan NL and Hiasa H: Topoisomerases as anticancer targets. Biochem J 475: 373-398, 2018.

31. Liu Q, Zhang Y, Liu S, Liu Y, Yang X, Liu G, Shimizu T, Ikenaka K, Fan K and Ma J: Cathepsin C promotes microglia M1 polarization and aggravates neuroinflammation via activation of Ca^{2+}-dependent PKC/p38MAPK/NF-KB pathway. J Neuroinflammation 16: 10, 2019.

32. Tian L, Li W, Yang L, Chang N, Fan X, Ji X, Xie J, Yang L and Li L: Cannabinoid receptor 1 participates in liver inflammation by promoting M1 macrophage polarization via rhoA/NF-KB p65 and ERK1/2 pathways, respectively, in mouse liver fibrogenesis. Front Immunol 8: 1214, 2017.

33. Nawaz A, Aminuddin A, Kado T, Takikawa A, Yamamoto S, Tsuneyama K, Igarashi Y, Ikutani M, Nishida Y, Nagai Y, *et al*: CD206(+) M2-like macrophages regulate systemic glucose metabolism by inhibiting proliferation of adipocyte progenitors. Nat Commun 8: 286, 2017.

34. Ji J, Xue TF, Guo XD, Yang J, Guo RB, Wang J, Huang JY, Zhao XJ and Sun XL: Antagonizing peroxisome proliferator-activated receptor γ facilitates M1-to-M2 shift of microglia by enhancing autophagy via the LKB1-AMPK signaling pathway. Aging Cell 17: e12774, 2018.

35. Jaiswal A, Reddy SS, Maurya M, Maurya P and Barthwal MK: MicroRNA-99a mimics inhibit M1 macrophage phenotype and adipose tissue inflammation by targeting TNFα. Cell Mol Immunol 16: 495-507, 2019.

36. Hirayama D, Iida T and Nakase H: The phagocytic function of macrophage-enforcing innate immunity and tissue homeostasis. Int J Mol Sci 19: E92, 2017.

37. Huber-Ruano I, Raventos C, Cuartas I, Sánchez-Jaro C, Arias A, Parra JL, Wosikowski K, Janicot M and Seoane J: An antisense oligonucleotide targeting TGF-β2 inhibits lung metastasis and induces CD86 expression in tumor-associated macrophages. Ann Oncol 28: 2278-2285, 2017.

38. Chen Y, Zhang S, Wang Q and Zhang X: Tumor-recruited M2 macrophages promote gastric and breast cancer metastasis via M2 macrophage-secreted CHI3L1 protein. J Hematol Oncol 10: 36, 2017.

39. Haque A, Moriyama M, Kubota K, Ishiguro N, Sakamoto M, Chinju A, Mochizuki K, Sakamoto T, Kaneko N, Munemura R, *et al*: CD206+ tumor-associated macrophages promote proliferation and invasion in oral squamous cell carcinoma via EGF production. Sci Rep 9: 14611, 2019.

40. Wynn TA, Chawla A and Pollard JW: Macrophage biology in.development, homeostasis, and disease. Nature 496: 445-455, 2013.

41. Song Y, Tang C and Yin C: Combination antitumor immunotherapy with VEGF and PIGF siRNA via systemic delivery of multi-functionalized nanoparticles to tumor-associated macrophages and breast cancer cells. Biomaterials 185: 117-132, 2018.

42. Tjiu JW, Chen JS, Shun CT, Lin SJ, Liao YH, Chu CY, Tsai TF, Chiu HC, Dai YS, Inoue H, *et al*: Tumor-associated macrophage-induced invasion and angiogenesis of human basal cell carcinoma cells by cyclooxygenase-2 induction. J Invest Dermatol 129: 1016-1025, 2009.

43. Lu C, Rong D, Zhang B, Zheng W, Wang X, Chen Z and Tang W: Current perspectives on the immunosuppressive tumor microenvironment in hepatocellular carcinoma: Challenges and opportunities. Mol Cancer 18: 130, 2019.

44. Sica A, Erreni M, Allavena P and Porta C: Macrophage polarization in pathology. Cell Mol Life Sci 72: 4111-4126, 2015.

45. Kubota K, Moriyama M, Furukawa S, Rafiul HASM, Maruse Y, Jinno T, Tanaka A, Ohta M, Ishiguro N, Yamauchi M, *et al*: CD163+CD204+ tumor-associated macrophages contribute to T cell regulation via interleukin-10 and PD-L1 production in oral squamous cell carcinoma. Sci Rep 7: 1755, 2017.

46. Lopez Nadal A, Peggs D, Wiegertjes GF and Brugman S: Exposure to antibiotics affects saponin immersion-induced immune stimulation and shift in microbial composition in zebrafish larvae. Front Microbiol 9: 2588, 2018.

47. Orihuela R, McPherson CA and Harry GJ: Microglial M1/M2 polarization and metabolic states. Br J Pharmacol 173: 649-665, 2016.

48. Anuforom O, Wallace GR, Buckner MM and Piddock LJ: Ciprofloxacin and ceftriaxone alter cytokine responses, but not Toll-like receptors, to Salmonella infection in vitro. J Antimicrob Chemother 71: 1826-1833, 2016.

49. Genin M, Clement F, Fattaccioli A, Raes M and Michiels C: M1 and M2 macrophages derived from THP-1 cells differentially modulate the response of cancer cells to etoposide. BMC Cancer 15: 577, 2015.

50. Zhang F, Parayath NN, Ene CI, Stephan SB, Koehne AL, Coon ME, Holland EC and Stephan MT: Genetic programming of macrophages to perform anti-tumor functions using targeted mRNA nanocarriers. Nat Commun 10: 3974, 2019.
51. Oliphant CM and Green GM: Quinolones: A comprehensive review. Am Fam Physician 65: 455-464, 2002.
52. Buckner MMC, Ciusa ML and Piddock LJV: Strategies to combat antimicrobial resistance: Anti-plasmid and plasmid curing. FEMS Microbiol Rev 42: 781-804, 2018.
53. Wang Y, Zhang Y, Wang Z, Zhang J, Qiao RR, Xu M, Yang N, Gao L, Qiao H, Gao M and Cao F: Optical/MRI dual-modality imaging of M1 macrophage polarization in atherosclerotic plaque with MARCO-targeted upconversion luminescence probe. Biomaterials 219: 119378, 2019.
54. Di Benedetto P, Ruscitti P, Vadasz Z, Toubi E and Giacomelli R: Macrophages with regulatory functions, a possible new therapeutic perspective in autoimmune diseases. Autoimmun Rev 18: 102369, 2019.
55. Lumeng CN, Bodzin JL and Saltiel AR: Obesity induces a phenotypic switch in adipose tissue macrophage polarization. J Clin Invest 117: 175-184, 2007.